Selective Inhibition of Trypanosomal Glyceraldehyde-3-phosphate Dehydrogenase by Protein Structure-Based Design: Toward New Drugs for the Treatment of Sleeping Sickness

Christophe L. M. J. Verlinde,*,† Mia Callens,§ Serge Van Calenbergh,⊥ Arthur Van Aerschot,‡ Piet Herdewijn,⊥,‡ Véronique Hannaert,§ Paul A. M. Michels,§ Fred R. Opperdoes,§ and Wim G. J. Hol†

Department of Biological Structure, and Biomolecular Structure Program, SM-20, School of Medicine, University of Washington, Seattle, Washington 98195, International Institute for Cellular and Molecular Pathology, Research Unit for Tropical Diseases, Brussels, Belgium, Laboratory of Medicinal Chemistry, University of Ghent, Belgium, and Rega Institute, Catholic University of Leuven, Belgium

Received April 28, 1994®

Within the framework of a project aimed at rational design of drugs against diseases caused by trypanosomes and related hemoflagellate parasites, selective inhibitors of trypanosomal glycolysis were designed, synthesized, and tested. The design was based upon the crystallographically determined structures of the NAD:glyceraldehyde-3-phosphate dehydrogenase complexes of humans and *Trypanosoma brucei*, the causative agent of sleeping sickness. After one design cycle, using the adenosine part of the NAD cofactor as a lead, the following encouraging results were obtained: (1) a 2-methyl substitution, targeted at a small pocket near Val 36, improves inhibition of the parasite enzyme 12.5-fold; (2) an 8-(thien-2-yl) substitution, aimed at Leu 112 of the parasite enzyme, where the equivalent residue in the mammalian enzyme is Val 100, results in a 167-fold better inhibition of the trypanosomal enzyme, while the inhibition of the human enzyme is improved only 13-fold; (3) exploitation of a "selectivity cleft" created by a unique backbone conformation in the trypanosomal enzyme near the adenosine ribose yields a considerable improvement in selectivity: 2′-deoxy-2′-(3-methoxybenzamido)adenosine inhibits the human enzyme only marginally but enhances inhibition of the parasite enzyme 45-fold when compared with adenosine. The designed inhibitors are not only better inhibitors of *T. brucei* GAPDH but also of the enzyme from *Leishmania mexicana*.

Introduction

Sleeping sickness is considered by the World Health Organization as one of the major tropical parasitic diseases.[1] It is caused by the protozoon *Trypanosoma brucei* and is always fatal if untreated. Current chemotherapy of sleeping sickness is unsatisfactory. Pentamidine and suramin are only useful in the early stages of the infection.[1] Melarsoprol is used in late-stage disease but frequently leads to fatal side effects.[2] The recently introduced drug eflornithine also has serious drawbacks: (i) it is less active against the more virulent *rhodesiense* form of the parasite,[3] (ii) resistance has already been reported,[4] (iii) treatment requires the intravenous administration of large quantities under hospitalization of the patient (the FDA recommends the daily administration of 400 mg/kg of body weight).[5] Clearly, more effective and safer drugs for the treatment of sleeping sickness are eagerly awaited.

T. brucei exhibits several most unusual features which can be exploited for rational drug design.[6] One of them is the dependence of the bloodstream form on glycolysis to the stage of pyruvate as a sole of energy supply.[7] Moreover, trypanosomes carry out glycolysis in a specialized organelle, the glycosome,[8] and consume glucose 50 times faster than human erythrocytes.[9] Therefore, we have chosen several of these glycosomal enzymes[10,11] as targets for protein structure-based inhibitor design. Obviously, such inhibitors will have to be selective and exhibit minimal affinity for the equivalent enzymes of the human host.

The design of selective active-site inhibitors is difficult because the active site of an enzyme is often well-conserved in the course of evolution. This is certainly true in the case of glycolytic enzymes.[12] In contrast, selective inhibition may be easier in case an enzyme makes use of a large cofactor, e.g., NAD. A substantial part of such a cofactor is not directly involved in the catalytic reaction, and as a consequence, its protein environment is less conserved. Following this principle, we report here on the successful design of selective inhibitors for glycosomal glyceraldehyde 3-phosphate dehydrogenase (gGAPDH, EC 1.2.1.12) of *T. brucei* based on the adenosine part of NAD as observed in the three-dimensional structures of trypanosomal as well as human GAPDH.[11]

T. brucei is closely related to other trypanosomatidae that are responsible for major tropical diseases, namely *Trypanosoma cruzi*, the causative agent of Chagas' disease, and several *Leishmania* species. We also present here evidence that the inhibitors we developed for *T. brucei* GAPDH may be of relevance for leishmaniasis and Chagas' disease.

Selective Inhibitor Design

The amino acid sequences of gGAPDH from *T. brucei* and human GAPDH are 55% identical.[12] Comparison of the three-dimensional structures of trypanosomal

* To whom correspondence should be addressed.
† University of Washington.
§ International Institute for Cellular and Molecular Pathology.
⊥ University of Ghent.
‡ Catholic University of Leuven.
® Abstract published in *Advance ACS Abstracts*, September 1, 1994.

0022-2623/94/1837-3605$04.50/0

Figure 1. Superposition of glycosomal GAPDH from *T. brucei* and human GAPDH. Only one subunit of the homotetrameric enzyme is shown, and the lines represent a smooth coil winding trough Cα positions. The ball-and-stick model shows the NAD cofactor as bound by the glycosomal GAPDH. Apart from two insertions, labeled as I-1 and I-2, the largest difference between the two enzymes occurs in a loop near the adenosine part of the NAD cofactor, labeled as Δ. This figure as well as Figures 2a, 3a, 4, and 5 were produced with the program MOLSCRIPT.[43]

gGAPDH[11] and human GAPDH[13,14] reveals that the NAD binding region is well-conserved around the nicotinamide part of the cofactor, i.e., the closest significant amino acid differences are between 7.5 and 14.5 Å away from the nicotinamide–ribose moiety. In contrast, the adenosine binding region shows structural differences between the parasite and human enzyme much closer to the cofactor (Table 1, supplementary material). In addition, the protein backbone adopts a quite different conformation in the immediate vicinity of the adenosine ribose 02′ (Figure 1). Therefore, our design strategy focused on adenosine as a molecular scaffold.

Before modifying adenosine we analyzed its binding mode to gGAPDH (Figure 2). The adenine ring is nicely sandwiched between Met 38 and Ala 89 on one side and Thr 110 and Leu 112 on the other side. It is further kept in place by a direct hydrogen bond between N6 and the backbone carbonyl of Gln 90 and presumably a water-mediated hydrogen bond between N1 and the backbone NH of Gln 90. Since the 3.2 Å Laue structure of glycosomal GAPDH does not allow an unequivocal interpretation of solvent molecules, the presence of the water molecule was inferred by analogy from the 1.8 Å crystal structure of *Bacillus stearothermophilus* GAPDH.[15] From the hydrogen-bonding scheme of the adenine ring we concluded that N1 and N6 substitutions tentatively could be excluded from design strategies. The ribose ring, which exhibits C2′-*endo* puckering, forms two good hydrogen bonds with the carboxylate of Asp 37. As a sequence alignment shows that this Asp is highly conserved in 47 GAPDH sequences,[12] it appeared logical to design only adenosine analogues which would retain these hydrogen bonds. It is also worth mentioning that the phosphate group attached to the adenosine moiety in NAD points with its two free oxygens toward the solvent and makes no direct interactions with the enzyme. Hence, we did not expect any additional benefit from designing AMP rather than adenosine analogues. Moreover, introducing a charged phosphate group may create an additional problem for the drug to cross membranes and to reach the enzyme inside the glycosome.

Subsequently, our design strategy focused on the three areas involved in the binding of the adenosine moiety where major differences between trypanosomal (Figure 2) and human GAPDH occur (Figure 3). Close to C-2 of the adenine ring gGAPDH has a hydrophobic residue, Val 36, instead of the hydrophilic Asn 33 in human GAPDH. Moreover, the packing around C-2 is rather loose and reveals a small pocket. Force-field calculations showed that gGAPDH could accommodate a methyl substituent on C-2 (compound **2**) at the expense of a small in-plane movement of the adenine ring and a concomitant weakening of the hydrogen bond at N6. Larger hydrophobic substituents like ethyl or thiomethyl appeared to be sterically unacceptable.

The second area of interest is the region near N-7 and C-8 of adenine. There the side chain of Leu 112 comes 1.0 Å closer to the adenine ring than the equivalent smaller residue of human GAPDH, Val 100. Any hydrophobic substituent which packs nicely against the side chain of Leu 112 should therefore provide some gain in selectivity in addition to a substantial gain in affinity. Because of synthetic convenience, our efforts concentrated on the design of C-8 derivatives. Modeling showed that a thien-2-yl substituent (compound **3**) packed well against the Leu 112 side chain, with CD1 and CD2 being buried in the interface. In this model the thienyl substituent is rotated 39° out of the plane of the adenine ring.

Finally, we explored the possibilities for creating selective inhibitors by exploiting the different protein backbone conformation near the adenosine ribose O2′. The difference occurs after the conserved Asp that interacts with the ribosyl hydroxyls. It includes residues Met 38–Tyr 44 in gGAPDH and Pro 35–Tyr 41 in human GAPDH. Where the human GAPDH backbone stays close to the ribose ring, the gGAPDH backbone diverges by as much as 6.0 Å at the third residue past the Asp. This difference is probably caused by the fact that the residue just after the conserved Asp is a proline in human GAPDH while it is a methionine in gGAPDH. Whereas the Met backbone N makes a hydrogen bond with the side chain of the conserved Asp, the Pro backbone nitrogen has no hydrogen bond donor capabilities. As a result the ψ angle of the Asp changes from −171° in gGAPDH to 105° in human GAPDH, ultimately leading to a different loop conformation. Therefore, only gGAPDH exhibits a cleft starting at the ribosyl hydroxyls and ending at the side chain of Asn 39. In view of the importance of this feature in the design process, we refer to this region as the "selectivity cleft."

The cleft in the glycosomal enzyme is largely hydrophobic due to the presence of Met 38 on one side and Val 205 of another subunit of the GAPDH tetramer on the other side. As the ribosyl 2′-hydroxyl projects right into the cleft, it offers the best starting point for making derivatives that would occupy this area which is, in human GAPDH, largely occupied by the side chain of Ile 37. However, merely using 2′-hydroxyl derivatives such as esters or ethers would deprive the conserved Asp from a hydrogen bonding partner and therefore, diminish the affinity for the enzyme dramatically. One way to overcome this problem is to replace the ribose 2′-hydroxyl by a 2′-amino function. Upon derivatization to an amide one then retains the hydrogen bond donor properties while, as an additional advantage, the synthetic coupling possibilities are ample. Force-field

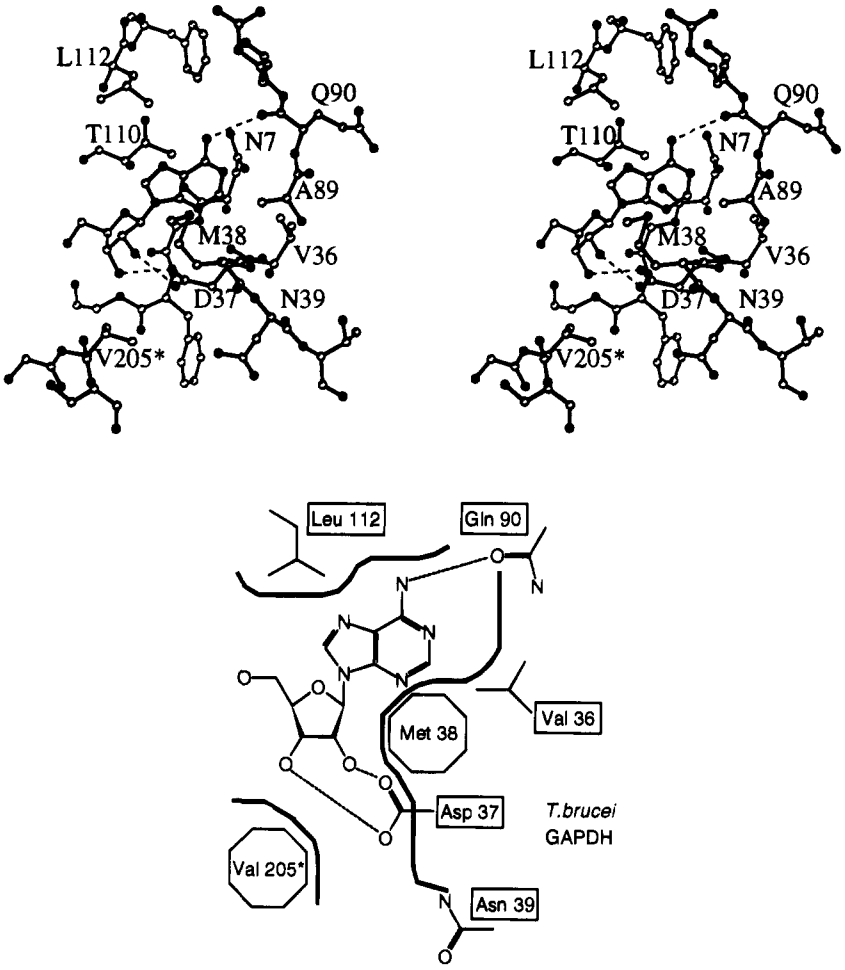

Figure 2. (a, Top) Stereofigure showing the binding mode of the adenosine part of NAD to glycosomal GAPDH of *T. brucei*. Hydrogen bonds are in dashed lines. (b, Bottom) Schematic diagram showing the binding mode of the adenosine part of NAD to *T. brucei* GAPDH, highlighting the residues that differ from human GAPDH.

calculations confirmed this view: a good hydrogen bond to Asp 37 is formed, the amide carbonyl points into solvent, and substituents on the carbonyl side reside in the "selectivity cleft". Due to the narrowness of this cleft we only modeled benzamide (compound **5**) and derivatives thereof. Our modeling suggested that hydrogen bond acceptors in the *meta* position of the benzyl moiety would hydrogen bond to the ND2 atom of the side chain of Asn 39 (as protein crystallography cannot distinguish between O and N atoms we inferred the ND2 identity from the observation that OD1 makes a hydrogen bond to the backbone N atom of Asp 41). A *m*-methoxy substituent (compound **7**) appeared to meet our criteria (Figure 4).

Although our design efforts focussed on glycosomal GAPDH from *T. brucei* sequence alignments make it clear that the inhibitor modeling may also be valid for glycosomal GAPDH from *Leishmania mexicana*[16] and *T. cruzi*.[17] These enzymes possess 81 and 90% sequence identity to *T. brucei* gGAPDH. Moreover, their local sequences responsible for binding adenosine and targeted at for inhibitor design are completely identical, with the single exception of a Ser in *L. mexicana* corresponding to Asn 39 in *T. brucei* (Table 2, supplementary material). Modeling showed that this difference, which would only be a matter of concern for the binding mode of compound **7**, has no real consequences since the hydroxyl of Ser can substitute for the hydrogen bond donor ability of ND2 from Asn 39.

Synthesis

The synthesis of compounds **2**[18] and **5**–**7**[19] has been fully described previously.

8-(Thien-2-yl)adenosine (**3**) and 8-phenyladenosine (**4**) were prepared analogously to the synthesis of other 8-alkylated adenosine derivatives[18] (Scheme 1). However, the more active catalyst triphenylarsine[20] was used for the cross-coupling reaction. Reaction of the 8-bromo analogue **8**[21] with 2-(tributylstannyl)thiophene at 80 °C followed by deacylation afforded **3** in 49% yield. The reaction with tetraphenyltin went more sluggishly and afforded the desired product **4** in 33% yield only.

Inhibition Studies

For all compounds synthesized the IC50 values for the inhibition of human, glycosomal *T. brucei* and glycosomal *L. mexicana* GAPDH are reported in Table 3. The inhibitory potency of adenosine (compound **1**) was determined for comparison. Apart from the designed compounds, two "isosteric" synthetic variants of the designed molecules were tested: the thienyl of **3** was replaced by phenyl in **4**, and the phenyl of **5** by a thienyl in **6**.

Results

From Table 3 it is apparent that our lead compound, adenosine (**1**), is a poor inhibitor of both parasite and human GAPDH. It is actually "antiselective" as it

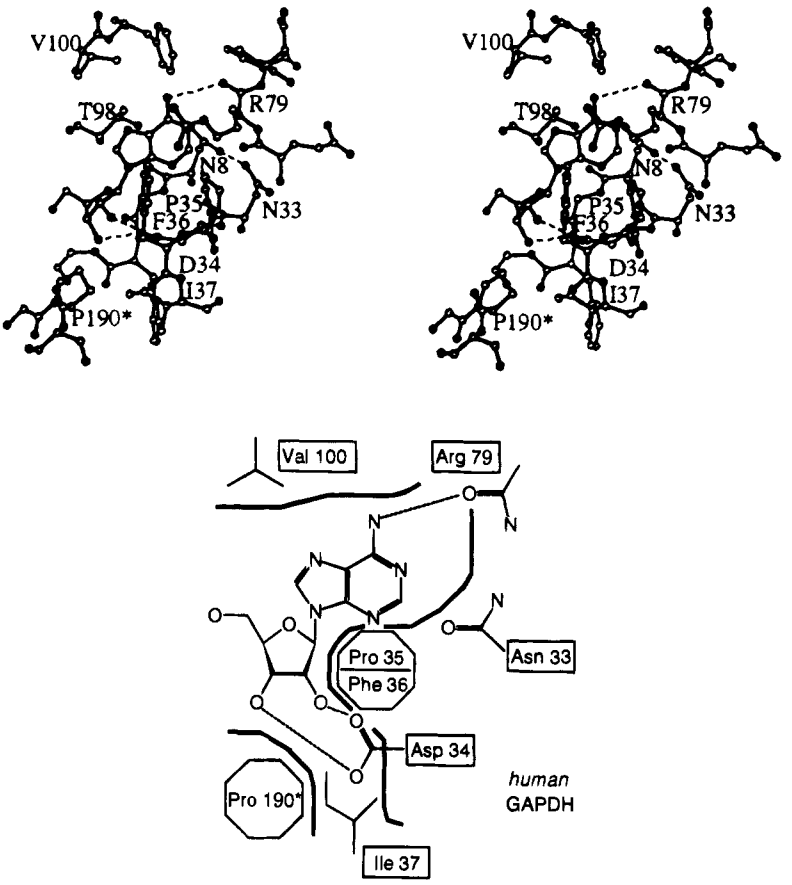

Figure 3. (a, Top) Stereofigure showing the binding mode of the adenosine part of NAD to human GAPDH. Hydrogen bonds are in dashed lines. (b, Bottom) Schematic diagram showing the binding mode of the adenosine part of NAD to human GAPDH, highlighting the residues that differ from *T. brucei* GAPDH.

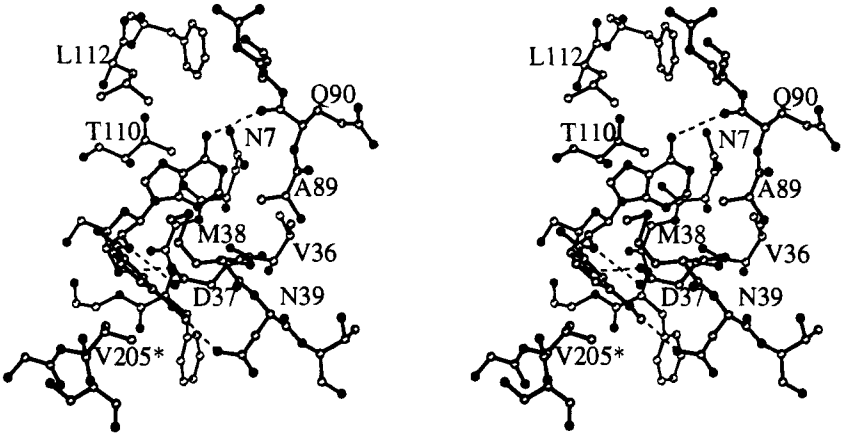

Figure 4. Stereofigure showing the modeled binding mode of 2′-deoxy-2′-(3-methoxybenzamido)adenosine to glycosomal GAPDH of *T. brucei*. Note the good fit of the benzamide ring between Met 38 and Val 205 of a neighboring subunit.

inhibits the human enzyme better than *T. brucei* gGAPDH. Introduction of a methyl group at position 2 of the adenine ring improves the inhibition of parasite enzyme substantially: over 12-fold for *T. brucei* and 8-fold for *L. mexicana*. Some selectivity is gained as the improvement for inhibiting human GAPDH is at most 3.5-fold. A more precise evaluation is unfortunately precluded by insolubility problems.

The introduction of a thien-2-yl at position 8 of the adenine ring yields more impressive results. Compound **3** inhibits *T. brucei* GAPDH 167 times better than adenosine. A somewhat smaller, 100-fold improvement is observed for *L. mexicana* GAPDH. The selectivity gain is modest, however, as the compound also inhibits human GAPDH 27 times better. Replacing thien-2-yl with phenyl (compound **4**) results in a loss of 1 order of magnitude in inhibitory activity toward both parasite and human enzyme.

Real gain in selectivity is obtained with the designed substituents on the ribosyl C2′. Compound **5**, with a benzamido substituent, inhibits *T. brucei* GAPDH 17 times better than adenosine, and the *L. mexicana* enzyme 15 times better. Similar results are observed when phenyl is replaced with thien-2-yl. Further derivatization of the phenyl ring with 3-methoxy leads to an inhibitor 45 times more effective than adenosine toward *T. brucei* and a spectacular 167 times toward *L. mexicana* GAPDH. As expected, the effect on human

Scheme 1

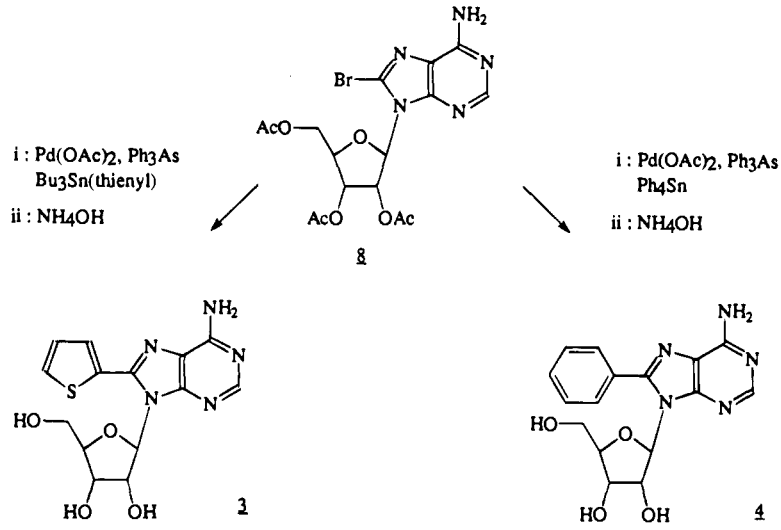

Table 3. Inhibitory Activities of Adenosine Derivatives toward Parasite and Human GAPDH (IC_{50}, mM)

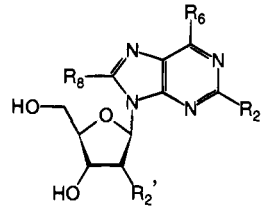

no.	R_2	R_8	$R_{2'}$	g. *T.b.*[a]	g. *L.m.*[b]	human[c]
1	H	H	OH	100	50	35
2	CH_3	H	OH	8	6	>10 [58%][d]
3	H	thien-2-yl	OH	0.6	0.5	1.3
4	H	phenyl	OH	10	ND[e]	10
5	H	H	NHCO-phenyl	6	3.3	>10 [100%][d]
6	H	H	NHCO-(thien-2-yl)	5	2.4	>10 [88%][d]
7	H	H	NHCO-(*m*-OCH_3-phenyl)	2.2	0.3	>10 [84%][d]

[a] g. *T.b.* = glycosomal *Trypanosoma brucei*. [b] g. *L.m.* = glycosomal *Leishmania mexicana*. [c] Human erythrocyte. [d] Not tested above the stated level due to insolubility, with the remaining activity at that level given in brackets. [e] ND = not determined.

GAPDH goes in the opposite direction: only marginal inhibition is obtained with compounds **5**–**7**.

Discussion

Our results clearly demonstrate that in one cycle of protein structure-based inhibitor design the inhibitory potency of a lead compound can readily be improved 10–170-fold. Moreover, several inhibitors exhibit the predicted selectivity for the parasite enzyme. As mentioned above our predictions were qualitative. For future design, however, it is of considerable interest to investigate how accurately our current computational scoring scheme reproduces the observed enhancement factors, even though we do not yet have experimental structures of the new inhibitors in complex with the target enzyme.

For the current series of inhibitors four factors determine the relative affinity: (i) the strain introduced in the ligand upon binding, (ii) changes in the strength of hydrogen bonds, (iii) steric clashes with the protein, and (iv) hydrophobic interactions. Two other factors affecting ligand affinity in general, loss of internal rotational entropy and electrostatic effects, were left out from our analysis because of the following considerations. First, the extra rotatable bonds introduced in compounds **3**–**7** involve conjugated systems that are also in solution sterically restrained by the adenosine system. In addition, the rotational possibilities of 8-thienyl and 8-phenyl are further limited due to partial conjugation with the adenine ring π system. Only for the methoxy group of compound **7**, which behaves essentially as a 2-fold rotor, a small correction for loss of entropy was applied. Second, none of the newly introduced substituents on adenosine contains charged groups. Hence, to a good approximation we can ignore the electrostatic interactions in our comparison of adenosine and its derivatives when bound to gGAPDH.

How well our current computational scoring scheme reproduces the observed enhancement factors is shown in Table 4. It shows an analysis of calculated inhibition enhancement factors relative to adenosine in terms of the four factors we consider important for binding and compares them with the observed *T. brucei* GAPDH inhibition. Care should be taken when interpreting individual components of the calculated binding energy resulting from the force-field calculations as they may vary slightly between different force fields. A few effects are nevertheless prominent. The 2-methyl group of compound **2** cannot be fully accommodated in the confined protein environment as is clear from the steric clashes and the loss of hydrogen bond energy. The latter occurs in essence around atoms N1 and N6 of the inhibitor. In contrast, the adenosine substituents on

Table 4. Calculated versus Observed *T. brucei* GAPDH Inhibition Enhancement Factors Relative to Adenosine

	kcal/mol						
no.	strain[a]	HB[b]	SC[c]	HE[d]	sum[e]	calc[f]	obs[g]
2	+0.1	+1.2	+0.9	−0.5 (28)	+1.7	0.06	12.5
3	−0.9	−1.0	+0.3	−1.1 (45)	−2.7	97	167
4	−0.4	−0.8	+0.0	−0.8 (32)	−2.0	30	10
5	−0.2	+0.6	+1.1	−2.8 (112)	−1.3	9.0	16.7
6	−0.7	+0.1	+1.6	−2.6 (103)	−1.6	15	20
7	−0.4	−0.2[h]	+2.8	−3.5 (138)	−1.9[i]	25	45

[a] Internal potential energy gain upon removal of the protein. [b] Hydrogen bond energy between protein and ligand; the energy involving the explicitly modeled water molecule, bound to N1, was also included. [c] Steric clashes. [d] Hydrophobic effect; the buried hydrophobic surface is given in parentheses. [e] Sum = strain + HB + HE + SC. [f] Calculated inhibition enhancement factor at 25 °C = 10 × exp(sum/−1.36). [g] Observed inhibition enhancement factor relative to adenosine. [h] Includes an estimated −1.5 kcal/mol[36] for the extra hydrogen bond made by the methoxy group. [i] Includes a +0.4 kcal/mol entropy penalty for freezing out one of the 2 possible coplanar conformations of the methoxy group.

position 8, exemplified by compounds **3** and **4**, are not constrained on all sides by the protein environment and do not exhibit steric clashes. In addition, they reinforce the fit of the inhibitors as the quality of the hydrogen bonds improves. Compounds **5**−**7** all occupy the unique cleft of the *T. brucei* GAPDH near the ribosyl C2′. Their fit is, however, not perfect as can be seen from the substantial steric clashes combined with a loss of hydrogen bond quality. Simply summing up the energies from the force-field calculations, i.e., factors i−iii, would thus predict that compounds **3** and **4** are better inhibitors than the lead compound while **2** and **5**−**7** are much worse, contradictory to the experimental inhibition data (Table 4).

The common characteristic of our designed adenosine analogues, however, is that they exploit the presence of hydrophobic areas on the protein surface. Calculations of the amount of hydrophobic area that is buried in the enzyme−inhibitor complex by the introduction of the new substituents should thus supplement the force-field calculations in order to obtain a fair indication of the gain in affinity. Even with a conservative estimate of the hydrophobic effect, 25 cal mol^{-1} Å^{-2},[22] considerable stabilizing energy contributions are calculated for all inhibitors. For compounds **5**−**7** the hydrophobic effect overcomes easily the destabilizing effect of the steric clashes. If we combine the hydrophobic effect with the force-field calculations (Table 4), the agreement between calculated and observed inhibition enhancement factors for compounds **3**−**7** is quite impressive: the biggest deviation is a factor of 3. It is quite puzzling why compound **2**, where the discrepancy is a factor 200, does not fit in this model. Three possible reasons can be listed. One, the combination of force-field with hydrophobic effect calculations is not adequate. This is difficult to believe since this protocol does a good job for the five other inhibitors. Two, the model overlooks the possibility of a *syn* rather than an *anti* conformation being bound. Modeling shows, however, that in the *syn* conformation the 2-methyl group remains fully solvent exposed upon binding, while the hydrogen bonds at N1 and N6 are lost. Therefore, this alternative binding mode cannot explain why the binding improves, unless there would be major conformational changes of the protein. Three, a partially unhappy water molecule may occupy the position of the 2-methyl group of compound **2** when adenosine is bound to gGAPDH. This unhappiness would originate from the fact that it can only form one hydrogen bond, namely with the water molecule bound to N1 of the adenine ring. The release of this water molecule by compound **2** would allow it to make at least two extra hydrogen bonds with the bulk solvent. This could easily account for the discrepancy factor of 200, corresponding to 3.1 kcal mol^{-1}, in our calculations. Eventually, only a structure determination of the inhibitor−enzyme complex may resolve this issue.

Despite the good agreement between calculation and observation for the five compounds, the modeled binding mode of the 8-substituted adenosine derivatives might be questioned. In small molecule crystal structures adenosine derivatives with a bulky 8-substituent (e.g., bromo) often exhibit a *syn* conformation about the glycosidic bond rather than the *anti* conformation of our model.[23] Could 8-(thien-2-yl)adenosine bind in the *syn* conformation to *T. brucei* GAPDH? Three arguments plead against this hypothesis. One, compared to anti the *syn* arrangement leads to 1.9 kcal/mol more strain, the loss of the hydrogen bonds formed with N1 and N6, 0.3 kcal/mol less steric clashes, and an extra 14.2 Å^2 buried hydrophobic surface. Even if the loss of hydrogen bonds would not be penalized, at most a 13-fold enhancement of inhibition over adenosine would be predicted, which is a factor 13 off the observed value. Two, C8 spin-labeled NAD and AMP do bind in the *anti* conformation to GAPDH despite bearing a bulky 4-amino-2,2,6,6-tetramethylpiperidin-1-oxyl group.[24,25] Three, a crystal structure determination for the analogous complex between horse liver alcohol dehydrogenase and 8-bromoadenosine diphosphoribose reveals and *anti* conformation despite a *syn* conformation in solution and in the small molecule crystal structure.[26] Thus, all evidence is in favor of an *anti* conformation for compounds **3** and **4**.

Another aspect of our design is that due to the nearly identical sequences in the inhibitor design region it should also apply to GAPDH of related parasites. It is pleasing to see that the inhibition enhancement factors we observe for *T. brucei* GAPDH are paralleled in the *L. mexicana* enzyme (Table 3). Except for compound **7** the discrepancy between these enhancement factors is at most a factor of 1.7. Another look at Table 2 (supplementary material) learns that compound **7** is actually the one where we expect a difference. Only this inhibitor tries to exploit the presence of Asn 39 in *T. brucei*, which has a Ser as counterpart in *L. mexicana*. Full understanding of the binding of inhibitor **7** will require at least the structure determination of the *L. mexicana* enzyme, which is, fortunately, well underway in our lab.[27]

In contrast to the marked increase of potency shown by our inhibitors toward parasite GAPDH, moderate to opposite effects are seen for inhibition of the human enzyme (Table 3). The best inhibition enhancement is observed for 8-(thien-2-yl)adenosine. This probably indicates that the thienyl group interacts to some extent with the Val 100 side chain in human GAPDH. The interaction is, however, less extensive than with the bigger Leu 112 side chain of the parasite enzyme. A more considerable degree of selectivity is obtained with

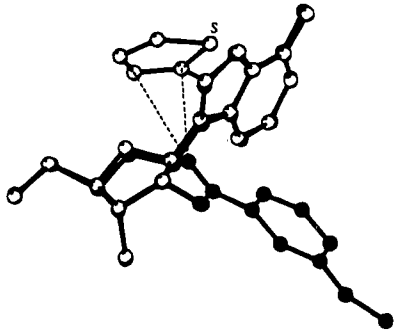

Figure 5. Superposition of 8-(thien-2-yl)adenosine (open representation) and 2′-deoxy-2′-(3-methoxybenzamido)adenosine (filled). Both molecules are in the modeled conformation when bound to the enzyme. Two dashed lines, each 3.2 Å long, between the amide oxygen atom of the benzamido substituent and C2 and C3 of the thienyl substituent, indicate the conformational incompatibility for combining the 8- and 2′-substituents in the same inhibitor.

inhibitors **5**–**7**, which exploit the "selectivity cleft" of the parasite GAPDH.

Future plans include further modification of the successful substituents, combining them in one molecule, thus leading to potentially much more potent and selective inhibitors, crystallographic determination of their complexes with parasite GAPDH, and testing against trypanosomes in vitro. It is rather unfortunate, however, that modeling already demonstrates that the 8-thienyl and 2′-(3-methoxybenzamido) substituents are incompatible when combined into one molecule. From Figure 5 it can be seen that the amide oxygen atom of the 2′-substituent would clash in the enzyme-bound conformation with the C2 and C3 atoms of the thienyl ring. However, if the substituent effects are additive, other combinations should produce inhibitors active in the micromolar range with a serious degree of selectivity.

The use of adenosine as a lead compound may have a fortuitous outcome as to the uptake of the inhibitors by trypanosomes. These parasites cannot synthesize purines and, therefore, have developed an active transport system for purines.[28] It is thus possible that our inhibitors might be taken up by these receptors. This mechanism is exploited by the experimental antitrypanosomal drug 5′-{[(*Z*)-4-amino-2-butenyl]methylamino}-5′-deoxyadenosine (MDL 73811), an irreversible inhibitor of *S*-adenosyl-L-methionine decarboxylase.[29] In addition, if our inhibitors would not be actively transported in the human host, which holds for MDL 73811, then their selectivity might be further enhanced. Testing of this hypothesis also forms part of our future plans.

Finally, we want to point out that pessimism about adenosine derivatives as drugs is not necessarily warranted. This doubt stems from the argument that many proteins recognize NAD(P), adenosine, and ATP. Cross-reactivity of adenosine derivatives with these different proteins and, therefore, toxicity may be expected. That this is not necessarily so is evident from the use of fludarabine, a C2′ epimer of adenosine, as an antileukemia agent with relatively low toxicity.[30] The much bigger changes to the adenosine scaffold in our inhibitors may hence lead to a surprisingly high overall selectivity.

Conclusions

The present work clearly demonstrates that even medium-resolution crystal structures can successfully be utilized for rational inhibitor design. Our studies also indicate that the concept of replacing the 2′-hydroxyl of adenosine by an amide for further coupling to a myriad of chemical fragments is a practical one. It may be of general application for exploiting differences near the 2′-hydroxyl position in a wide variety of nucleoside binding proteins in humans and pathogens.

Experimental Section

(1) Structural Data. The crystal structure of *T. brucei* gGAPDH has been determined from Laue data at a resolution of 3.2 Å; due to 6-fold density averaging of the 1.5-tetramer in the asymmetric unit the quality of the structure is better than what might normally be expected at this resolution.[11] All modeling was based on this structure. Recently, the structure of another crystal form of *T. brucei* gGAPDH has been determined at 2.8 Å resolution.[31] The two gGAPDH structures superimpose very well: the rms coordinate shift is 0.44 Å for 352 Cα residues (disordered N- and C-terminal residues 1–2 and 354–358 were omitted). The gGAPDH structure was compared with the structure of human muscle GAPDH,[13] for which the resolution was extended from 3.5 to 2.4 Å.[14]

The superposition of gGAPDH and human GAPDH was carried out in two stages. After an initial superposition based on the published alignment,[32] topologically equivalent Cα positions were determined by visual inspection on the graphics. A final least-squares calculation for the 303 selected Cα atoms resulted in an rms coordinate difference of 0.79 Å.

During the review process of this paper the crystal structure of *L. mexicana* gGAPDH has been determined.[27] Though the refinement has not yet been fully completed, the quality of the structure is already excellent: R = 19.0% (10.0–2.8 Å) with 157 water molecules in the model. Superposition of this gGAPDH onto *T. brucei* gGAPDH shows that the overall structure is nearly identical: the RMS deviation for all the backbone atoms is only 0.59 Å. The RMS deviation for all side chain atoms targeted for inhibitor design is 0.45 Å.

(2) Design and Molecular Modeling. Computer modeling was carried out by using the program BIOGRAF[33] in conjunction with the Dreiding force field.[34] Prior to synthesis qualitative docking experiments were carried out in a rigid protein environment. They consisted of modifying the adenosine moiety of the crystallographically observed NAD followed by conjugate gradient minimization (the energy minimization convergence criterion was set to 0.1 kcal mol^{-1} Å^{-1}). Since energy calculations were carried out in vacuo, the electrostatic term of the potential energy function was turned off. The most important effect of electrostatics, namely the formation of hydrogen bonds, was taken care of by explicit geometrical hydrogen bond potentials of the Lennard–Jones 12–10 type. This approach avoids the difficulties of calculating and calibrating charges for each new ligand, and of treating dielectric effects in detail.[35] For docking compounds **5**–**7** the side chain conformation of Met 38 was allowed to move in order to alleviate short contacts between CG and the aromatic ring system of the 2′-ribosyl substituents.

For quantitative analysis of the inhibition enhancement factors seen with our inhibitors the modeling protocol was elaborated as follows: (1) The water molecule hydrogen bonding to N1 inferred to be present by analogy to the *B. stearothermophilus* GAPDH structure[15] (see the section on selective inhibitor design) was added to the model. (2) All residues within 7.0 Å of the modeled inhibitor were allowed to move, while the remainder of the protein was kept fixed. (3) The hydrophobic effect was estimated for molecular surface calculations carried out with the program MS.[36] Extended atomic radii were taken from ref 37, and the probe radius was set to 1.4 Å. The magnitude of the hydrophobic effect was assumed to be 25 cal mol^{-1} Å^{-2}.[22] (4) Extra hydrogen bonds not present in the original GAPDH–adenosine complex were

assumed to contribute 1.5 kcal/mol to the binding.[38] This applied only to the methoxy of compound **7**.

(3) Synthesis. Ultraviolet spectra were recorded with a Philips PU 8700 UV/vis spectrophotometer. The ^1H and ^{13}C NMR spectra were determined with a JEOL FX 90Q spectrophotometer with tetramethylsilane as internal standard for the ^1H NMR spectra and DMSO-d_6 (39.6 ppm) for the ^{13}C NMR spectra. Electron impact (EI) mass spectra were obtained using a Kratos Concept ^1H mass spectrometer (fragment ion, relative intensity).

8-(Thien-2-yl)adenosine (3). To 5 mL of *N*-methylpyrrolidinone was added sequentially 472 mg (1.0 mmol) of **8**,[21] 22 mg (0.1 mmol) of palladium(II) acetate, 0.14 mL (1 mmol) of triethylamine, and 61 mg (0.2 mmol) of triphenylarsine. This mixture was stirred for 10 min at room temperature under a nitrogen blanket. Next, 0.75 of crude 2-(tributylstannyl)-thiophene (2 mmol) was added, and the mixture was heated at 80 °C overnight. TLC analysis (CH_3CN–EtOAc, 95:5) indicated the reaction to be complete. The mixture was then diluted with 50 mL of CH_2Cl_2 and washed with water (3 × 50 mL). The organic layer was dried (Na_2SO_4), concentrated, and purified on silica gel (CH_2Cl_2–MeOH, 99:1) to yield **3** as its triacetate (MS *m/z* 475; UV (MeOH) λ_{max} = 248, 303 nm). Ammonolysis with MeOH–dioxane–30% NH_3 (1:1:1) overnight at room temperature gave the title product **3** which was purified on silica gel (CH_2Cl_2–MeOH, 99:1) and crystallized from a methanol–dioxane mixture, affording 168 mg (0.49 mmol, 49% overall yield) of the title compound. UV (MeOH): λ_{max} 247 (15 550), 303 (16 600), λ_{min} 270 (8600) nm. ^1H NMR (DMSO-d_6): δ 3.63 (m, 2H, H-5′), 3.99 (m, 1H, H-4′), 4.21 (m, 1H, H3′), 5.18 (m, 2H, H2′, 3′-OH), 5.49 (br s, 2′-OH), 5.76 (br s, 5′-OH), 6.01 (d, 1H, J = 6.6 Hz, H-1′), 7.28 (t, 1H, H-4″), 7.50 (s, 2H, NH_2), 7.66 (d), 7.87 (d, H-3″, H-5″), 8.15 (s, 1H, H-2) ppm. ^{13}C NMR spectra (DMSO-d_6): δ 62.3 (C-5′), 71.1, 71.5 (C-2′, C-3′), 86.6 (C-4′), 89.2 (C-1′), 119.3 (C-5), 128.2, 130.0, 130.1 (C-3″, C-4″, C-5″), 130.7 (C-2″), 145.1 (C-8), 150.1 (C-4), 152.2 (C-2), 156.1 (C-6) ppm. MS (EI): *m/z* 349 (M^+, 8), 260 (217 + CHCHOH, 10), 217 (B + H, 100), 190 (217–HCN, 12). Anal. ($C_{14}H_{15}N_5O_4S_1$) C, H, N.

8-Phenyladenosine (4). To the reaction mixture as described for the preparation of **3** was added 854 mg (2 mmol) of tetraphenyltin. The mixture was heated at 110 °C for 16 h. Attempted purification on silica gel (CH_2Cl_2–MeOH, 99:1) yielded an unpure product which was deacylated as described for **3**. Two major products (R_f 0.30 and 0.36, respectively, ratio 3:2) were detected upon TLC analysis. They were separated on silica gel (CH_2Cl_2–MeOH, 95:5). The less polar one carried in addition to a phenyl a NMP substituent of which the correct structure could not been determined. The more polar one was crystallized from MeOH–Et_2O and a few drops of toluene, affording 115 mg (0.33 mmol, 33%) of the title product **4** as a hygroscopic solid. UV (MeOH) λ_{max} 230 (13 300), 281 (11 800), λ_{min} 248 (4020) nm. ^1H NMR (DMSO-d_6): δ 3.67 (m, 2H, H-5′), 3.96 (m, 1H, H-4′), 4.19 (dd, J = 5.3 Hz and 1.5 Hz, 1H, H3′), 5.13 (d, J = 4.4 Hz, 3′-OH), 5.20 (dd, J = 5.0 Hz and 7.0 Hz, H-2′), 5.48 (d, J = 6.5 Hz, 2′-OH), 5.77 (d, J = 7.5 Hz, H-1′), 5.82 (t, 5′-OH), 7.4–7.85 (m, arom H, NH_2), 8.16 (s, 1H, H-2) ppm. ^{13}C NMR spectra (DMSO-d_6): δ 62.4 (C-5′), 71.2, 71.4 (C-2′, C-3′), 86.8 (C-4′), 89.2 (C-1′), 119.2 (C-5), 128.8, 129.5, 129.7, 130.1 (arom), 149.9 (C-8), 151.1 (C-4), 152.1 (C-2), 156.3 (C-6) ppm. MS (EI): *m/z* 343 (M^+, **4**), 254 (211 + CHCHOH, 12), 217 (B + H, 100), 184 (211 − HCN, 8). Anal. ($C_{16}H_{17}N_5O_4S_1 \cdot 0.5H_2O$) C, H; N: calcd, 19.88; found, 19.17.

(4) Inhibition Studies. (a) Enzymes, Substrates, and Cofactors. Human erythrocyte glyceraldehyde-3-phosphate dehydrogenase was purchased from Sigma. Substrates and cofactors were purchased from Boehringer Mannheim or from Sigma. *T. brucei* and *L. mexicana* glycosomal GAPDHs have been obtained by overexpression in *Escherichia coli*. A number of physicochemical and kinetic properties of the purified recombinant enzymes[39] have been compared with those of the protein purified[40] from glycosomes of the parasite. For recombinant *T. brucei* gGAPDH the K_m (NAD) = 0.54 ± 0.06 mM. This is virtually indistinguishable from the values for the authentic enzyme: K_m (NAD) = 0.45 ± 0.18 mM. For recombinant *L. mexicana* gGAPDH the K_m (NAD) = 0.41 ± 0.03 mM. Again, this is practically indistinguishable from the value for the authentic enzyme: K_m (NAD) = 0.38 ± 0.04 mM. Details of the purification and characterization of the recombinant gGAPDHs will be published elsewhere.[41]

(b) Inactivation Studies. Compounds **1**–**7** were dissolved in 100% DMSO. The inactivation of GAPDH by the compounds was measured at 25 °C and at subsaturated concentrations of glyceraldehyde-3-phosphate and NAD. The reaction mixture contained 0.1 M triethanolamine–HCl buffer, pH 7.6, 1 mM dithiothreitol, 1 mM EDTA, 0.1 M KCl, 10 mM potassium phosphate, 0.8 mM glyceraldehyde-3-phosphate, and 0.4 mM NAD. The concentration of DMSO in the reaction cuvette was kept at 5%. The enzyme reaction was started by the addition of GAPDH. Possible effects of inhibitors on the absorbance of NADH were verified by running reactions without enzyme. The percentage of remaining activity was calculated from the initial reaction rate in the presence of the compound and the initial reaction rate under identical conditions without the compound but with 5% DMSO. For the calculation of IC50 values at least five concentrations of inhibitor were tested, causing 5–80% inhibition. Statistical error limits on the IC50 values[42] have been calculated to amount to 10%.

Acknowledgment. It is a pleasure to thank Drs. Fred M. D. Vellieux and Randy J. Read for the crystal structure determinations which made this work possible. We are also grateful to Dr. Jozef Rozenski for obtaining mass spectra and Mr. Van Roy for help with the inhibition studies. This research project was supported by the WHO/UNDP/World Bank Special Programme for Research and Training in Tropical Diseases, by the EEC Science and Technology Program for Development, and by a gift from Hoffmann–La Roche, Basel.

Supplementary Material Available: Table 1, significant amino acid differences between *T. brucei* gGAPDH and human GAPDH in the NAD binding pocket; Table 2, Alignment of parasite glycosomal GAPDH sequences in the adenosine binding region (2 pages). Ordering information is given on any current masthead page.

References

(1) Tropical Diseases. Progress in Research, 1989–1990. *Tenth Programme Report*. WHO: Geneva, 1991; pp 59–68.
(2) Haller, L.; Adams, H.; Merouze, F.; Dago, A. Clinical and pathological aspects of human African trypanosomiasis (*T. b. gambiense*) with particular reference to reactive arsenical encephalopathy. *Am. J. Trop. Med. Hyg.* **1986**, *35*, 94–99.
(3) *Tropical Drug Res. News* **1990**, No. 34, 1.
(4) Bellofatto, V.; Fairlamb, A.; Henderson, G. B.; Cross, G. A. M. Biochemical changes associated with α-difluoromethylornithine uptake and resistance in *Trypanosoma brucei*. *Mol. Biochem. Parasitol.* **1987**, *25*, 227–238.
(5) *Tropical Drug Res. News* **1991**, No. 35, 7.
(6) Hol, W. G. J.; Vellieux, F. M. D.; Verlinde, C. L. M. J.; Wierenga, R. K.; Noble, M. E. M.; Read, R. J. Crystallographic Investigations of Glycolytic Enzymes from *Trypanosoma brucei*: Potential Starting Points for the Design of New Sleeping Sickness Drugs. In *Molecular Conformation and Biological Interactions*; Balaram, P., Ramaseshan, S., Eds.; Indian Acad. Sci.: Bangalore, 1991; pp 215–244.
(7) Opperdoes, F. R. Compartmentation of Carbohydrate Metabolism in Trypanosomes. *Annu. Rev. Microbiol.* **1987**, *41*, 127–151.
(8) Opperdoes, F. R.; Borst, P. Localization of nine glycolytic enzymes in a microbody-like organelle in *Trypanosoma brucei*: the glycosome. *FEBS Lett.* **1977**, *80*, 360–364.
(9) Wang, C. C. Parasite enzymes as potential targets for antiparasitic chemotherapy. *J. Med. Chem.* **1984**, *27*, 1–9.
(10) Wierenga, R. K.; Kalk, K. H.; Hol, W. G. J. Structure Determination of the Glycosomal Triosephosphate Isomerase from *Trypanosoma brucei* at 2.4 Å Resolution. *J. Mol. Biol.* **1987**, *198*, 109–121.
(11) Vellieux, F. M. D.; Hajdu, J.; Verlinde, C. L. M. J.; Groendijk, H.; Read, R. J.; Greenhough, T. J.; Campbell, J. W.; Kalk, K. H.; Littlechild, J. A.; Watson, H. C.; Hol, W. G. J. Structure of glycosomal glyceraldehyde-3-phosphate dehydrogenase from *Trypanosoma brucei* determined from Laue data. *Proc. Natl. Acad. Sci. U.S.A.* **1993**, *90*, 2355–2359.

(12) Fothergill-Gilmore, L.; Michels, P. A. M. Evolution of glycolysis. *Prog. Biophys. Molec. Biol.* **1993**, *59*, 105–235.
(13) Mercer, W. D.; Winn, S. I.; Watson, H. C. Twinning in crystals of human skeletal muscle D-glyceraldehyde-3-phosphate dehydrogenase. *J. Mol. Biol.* **1976**, *250*, 277–283.
(14) Read, R. J. et al. Unpublished results.
(15) Skarzynski, T.; Moody, P. C. E.; Wonacott, A. J. Structure of the holo-Glyceraldehyde-3-phosphate Dehydrogenase from *Bacillus stearothermophilus* at 1.8 Å Resolution. *J. Mol. Biol.* **1987**, *193*, 171–187.
(16) Hannaert, V.; Blaauw, M.; Kohl, L.; Allert, S.; Opperdoes, F. R.; Michels, P. A. M. Molecular analysis of the cytosolic and glycosomal glyceraldehyde-3-phosphate dehydrogenase in *Leishmania mexicana*. *Mol. Biochem. Parasitol.* **1992**, *55*, 115–126.
(17) Kendall, G.; Wilderspin, A. F. W.; Ashall, F.; Miles, M. A.; Kelly, J. M. *Trypanosoma cruzi* glyceraldehyde-3-phosphate dehydrogenase does not conform to the "hotspot" model of topogenesis. *EMBO J.* **1990**, *9*, 2751–2758.
(18) Van Aerschot, A.; Mamos, P.; Weyns, N.; Ikeda, S.; De Clercq, E.; Herdewijn, P. Antiviral activity of C-alkylated purine nucleotides obtained by cross-coupling with tetraalkyltin reagents. *J. Med. Chem.* **1993**, *36*, 2938–2942.
(19) Van Calenbergh, S.; Van Den Eeckhout, E.; Herdewijn, P.; De Bruyn, A.; Verlinde, C.; Hol, W.; Callens, M.; Van Aerschot, A.; Rozenski, J. Synthesis and conformational analysis of 2′-deoxy-2′-(3-methoxybenzamido)adenosine, a rational-designed inhibitor of trypanosomal glyceraldehyde phosphate dehydrogenase. *Helv. Chim. Acta* **1994**, *77*, 631–644.
(20) Vittorio, F.; Bala, K. Large rate accelerations in the Stille reaction with tri-2-furylphosphine and triphenylarsine as Palladium ligands: Mechanistic and synthetic applications. *J. Am. Chem. Soc.* **1991**, *113*, 9585–9595.
(21) Ikehara, M.; Kaneko, K. Studies of nucleosides and nucleotides XLI: Purine cyclonucleosides - 8. Selective sulfonylation of 8-bromoadenosine derivatives and an alternate synthesis of 8,2′- and 8,3′-cyclonucleosides. *Tetrahedron* **1970**, *26*, 4215–4259.
(22) Chothia, C. Hydrophobic bonding and accessible surface area in proteins. *Nature* **1974**, *248*, 338–339.
(23) Saenger, W. *Principles of nucleic acid structure*; Springer-Verlag: New York, 1984; pp 76–78.
(24) Deparade, M. P.; Glöggler, K.; Trommer, W. E. Isolation and properties of glyceraldehyde-3-phosphate dehydrogenase from a sturgeon from the Caspian sea and its interaction with spin-labeled NAD^+ derivatives. *Biochem. Biophys. Acta* **1981**, *659*, 422–433.
(25) Karim, C.; Philipp, R.; Trommer, W. E.; Park, J. H. Interaction of glyceraldehyde-3-phosphate dehydrogenase with AMP as studied by means of a spin labeled analog. *Biol. Chem. Hoppe-Seyler* **1989**, *370*, 1245–1252.
(26) Abdallah, M. A.; Biellmann, J. F.; Nordström, B.; Bränden, C.-I. The conformation of adenosine diphosphoribose and 8-bromoadenosine diphosphoribose when bound to liver alcohol dehydrogenase. *Eur. J. Biochem.* **1975**, *50*, 475–481.
(27) Kim, H.; et al. Unpublished results.
(28) Hammond, D. J.; Gutteridge, W. E. Purine and pyrimidine metabolism in the *Trypanosomatidae*. *Mol. Biochem. Parasitol.* **1984**, *13*, 243–261.
(29) Byers, T. L.; Casara, P.; Bitonti, A. J. Uptake of the antitrypanosomal drug 5′-{[(*Z*)-4-amino-2-butenyl]methylamino}-5′-deoxyadenosine (MDL 73811) by the purine transport system of *Trypanosoma brucei brucei*. *Biochem. J.* **1992**, *283*, 755–758.
(30) Whelan, J. S.; Davis, C. L.; Rule, S.; Ranson, M.; Smith, O. P.; Metha, A. B.; Catovsky, D.; Rohatiner, A. Z.; Lister, T. A. (1991). Fludarabine phosphate for the treatment of low grade lymphoid malignancy. *Br. J. Cancer 64*, 120–123.
(31) Read, R. J.; et al. Unpublished results.
(32) Michels, P. A. M.; Poliszczak, A.; Osinga, K. A.; Misset, O.; Van Beeumen, J.; Wierenga, R. K.; Borst, P.; Opperdoes, F. R. Two tandemly linked identical genes code for the glycosomal glyceraldehyde-phosphate dehydrogenase in *Trypanosoma brucei*. *EMBO J.* **1986**, *5*, 1049–1056.
(33) Biograf 3.10; Molecular Simulations Inc., 16 New England Executive Park, Burlington, MA 01803–5297.
(34) Mayo, S. L.; Olafson, B. D.; Goddard, W. A., III. DREIDING: A Generic Force Field for Molecular Simulations. *J. Phys. Chem.* **1990**, *94*, 8897–8909.
(35) Mueller, K.; Amman, H.-J.; Doran, D. M.; Gerber, P. R.; Gubernator, K.; Schrepfer, G. The use of computer modeling and structural databases in pharmaceutical research. In *Trends in Medical Chemistry '88*; van der Goot, H., Domany, G., Pallos, L., Timmerman, H., Eds.; Elsevier Science Publishers: Amsterdam, 1989; pp 1–12.
(36) Connolly, M. L. Analytical molecular surface calculations. *J. Appl. Crystallogr.* **1983**, *16*, 548–558.
(37) McCammon, J. A.; Woylnes, P. G.; Karplus, M. Picosecond dynamics of tyrosine side chains in proteins. *Biochemistry* **1979**, *18*, 927–942.
(38) Shirley, B. A.; Stanssens, P.; Hahn, U.; Pace, C. N. Contribution of Hydrogen Bonding to the Conformational Stability of Ribonuclease T1. *Biochemistry* **1992**, *31*, 725–732.
(39) Lambeir, A.-M.; Loiseau, A. M.; Kuntz, D. A.; Vellieux, F. M.; Michels, P. A. M.; Opperdoes, F. R. The cytosolic and glycosomal glyceraldehyde-3-phosphate dehydrogenase from *Trypanosoma brucei*. *Eur. J. Biochem.* **1991**, *198*, 429–435.
(40) Misset, O.; Bos, O. J. M.; Opperdoes, F. R. Glycolytic enzymes of *Trypanosoma brucei*. Simultaneous purification, intraglycosomal concentrations and physical properties. *Eur. J. Biochem.* **1986**, *157*, 441–453.
(41) Hannaert, V.; et al. Unpublished results.
(42) Job, D.; Cochet, C.; Dhien, A.; Chambaz, E. M. A rapid method for screening inhibitor effects: determination of I50 and its standard deviation. *Anal. Biochem.* **1978**, *84*, 68–77.
(43) Kraulis, P. J. MOLSCRIPT: a program to produce both detailed and schematic plots of protein structures. *J. Appl. Crystallogr.* **1991**, *24*, 946–950.